Available online at www.sciencedirect.com

SCIENCE DIRECT®

ELSEVIER

Journal of Computational and Applied Mathematics 168 (2004) 471–479

JOURNAL OF COMPUTATIONAL AND APPLIED MATHEMATICS

www.elsevier.com/locate/cam

Validation of the integral model for the pyrolysis of charring materials with a moving grid

E. Theuns*, J. Vierendeels, P. Vandevelde

Department of Flow, Heat and Combustion Mechanics, Ghent University, Sint-Pietersnieuwstraat 41, Gent 9000, Belgium

Received 17 September 2002; received in revised form 19 June 2003

Abstract

For the pyrolysis of charring materials a new one dimensional moving grid model is developed. The solid is divided by a pyrolysis front into a char and a virgin layer. Only when the virgin material reaches a critical temperature it starts to pyrolyse. The progress of the pyrolysis front determines the release of combustible volatiles. Since the model is used here as a stand-alone model, the external heat flux that heats up the solid, is assumed to be known.

The char and virgin grid move along with the pyrolysis front. Calculations are done on uniform and nonuniform grids for the virgin layer. In the char layer only a uniform grid is used. Calculations done with a non-uniform grid are about 3 times faster than with a uniform grid.

The moving grid model is used to validate the approximate *integral model*. This revealed that the *integral model* gives significant errors when there are sudden changes in the boundary conditions.

Keywords: Pyrolysis; Moving grid; Char; Integral model

1. Introduction

In most of today's compartment fire models, i.e. zone and CFD models, the fire is still predefined. The progress of the fire is defined before the calculation and thus the reaction of the combustible materials is not coupled to the conditions in the enclosure. This gives serious restrictions. Models that can predict the fire growth itself, e.g. from a burning cigarette to a fully involved fire, would

* Corresponding author.
E-mail address: erwin.theuns@rug.ac.be (E. Theuns).

0377-0427/$ - see front matter
doi:10.1016/j.cam.2003.12.013

Nomenclature

a	mesh growth factor
c	specific heat capacity (J/kg K)
H_{pyr}	latent heat of pyrolysis (J/kg)
L	total thickness of solid (m)
$\dot{m}''$	mass flux (kg/m^2 s)
$\dot{q}''_c$	heat flux char to front (W/m^2)
$\dot{q}''_{net}$	net incident heat flux (W/m^2)
$\dot{q}''_v$	heat flux front to virgin (W/m^2)
T	temperature (K)
t	time (s)
w	mesh velocity (m/s)
x	distance from front surface (m)

Greek Letters

α	thermal diffusivity [m^2/s]
δ_c	thickness of char layer [m]
ε	emissivity of solid surface
θ	controls type of difference scheme
λ	thermal conductivity (W/m K)
ρ	density (kg/m^3)
σ	Stefan–Boltzmann constant (W/m K^4)

Subscripts

c	char
E	east or right node
g	pyrolysis gases
pyr	pyrolysis
s	surface
v	virgin
W	west or left node
∞	environment

expand substantially the utility of fire models. Therefore, a simple, fast and accurate solid pyrolysis model needs to be developed.

In aerospace engineering intensive work has been done in solid (propellant) combustion [2,4]. Also for fire applications there exist several solid combustion models. The models that describe the pyrolysis of charring materials go from simple analytical equations [12] to complex coupled partial differential equations where the thermal degradation reactions are modelled with a first order Arrhenius equation [7,11]. The moving grid model that will be described here, is faster than the Arrhenius models while the results are still accurate.

2. Physical model

The pyrolysis front is modelled as a surface with zero thickness. During pyrolysis the char and virgin zones are always separated from each other by this pyrolysis front. Each zone consists of only one material (virgin or char) and has constant thermal parameters. The temperature of the pyrolysis front is assumed a material property. The pyrolysis gases produced at the pyrolysis front, flow immediately out of the solid [10,13]. When the kinetic and the potential energy is neglected, the conservation of energy for the char layer for one dimensional pyrolysis gives

$$\frac{\mathrm{d}}{\mathrm{d}t}\int_0^{\delta_c} \rho_c c_c T \,\mathrm{d}x + \dot{m}''_g c_g T_s - \dot{m}''_g c_g T_{pyr} - (\rho_c c_c T_{pyr})\left(\frac{\mathrm{d}\delta_c}{\mathrm{d}t}\right) = \dot{q}''_{net} - \dot{q}''_c. \tag{1}$$

The boundary conditions for the char layer are

$$-\lambda_c \left.\frac{\mathrm{d}T}{\mathrm{d}x}\right|_{x=0} = \dot{q}''_{net} = \dot{q}''_{ext} + \dot{q}''_{flame} - \varepsilon\sigma(T_s^4 - T_\infty^4),$$

$$T|_{x=\delta_c} = T_{pyr} \tag{2}$$

with $\dot{q}''_{ext}$ and $\dot{q}''_{flame}$ the heat flux from an external heat source and from the flame respectively. In a similar way, the conservation equation of energy for the virgin material gives

$$\frac{\mathrm{d}}{\mathrm{d}t}\int_{\delta_c}^{L} \rho_v c_v T \,\mathrm{d}x + \rho_v c_v T_{pyr}\frac{\mathrm{d}\delta_c}{\mathrm{d}t} = \dot{q}''_v. \tag{3}$$

The back surface is insulated, thus the boundary conditions are

$$T|_{x=\delta_c} = T_{pyr},$$

$$\lambda_v \left.\frac{\mathrm{d}T}{\mathrm{d}x}\right|_{x=L} = 0. \tag{4}$$

The char layer and the virgin material are coupled with each other by the pyrolysis front at $x = \delta_c$. Although the pyrolysis front is assumed infinitely thin, the conservation equations are still applicable. The conservation of mass gives

$$(\rho_v - \rho_c)\frac{\mathrm{d}\delta_c}{\mathrm{d}t} = \dot{m}''_g. \tag{5}$$

At the pyrolysis front heat will be absorbed by the chemical degradation reactions. The conservation of energy gives

$$(\rho_v - \rho_c)\frac{\mathrm{d}\delta_c}{\mathrm{d}t}\Delta H_{pyr}(T_{pyr}) = \dot{q}''_c - \dot{q}''_v. \tag{6}$$

Similar equations have been derived by Moghtaderi et al. [9] and Spearpoint and Quintiere [10].

3. Numerical model with moving grid

3.1. Space discretization

During the pyrolysis phase the front temperature is known. It is the so-called pyrolysis temperature. As the virgin and the char layer both end at that front, a half-cell is taken so that a node can be

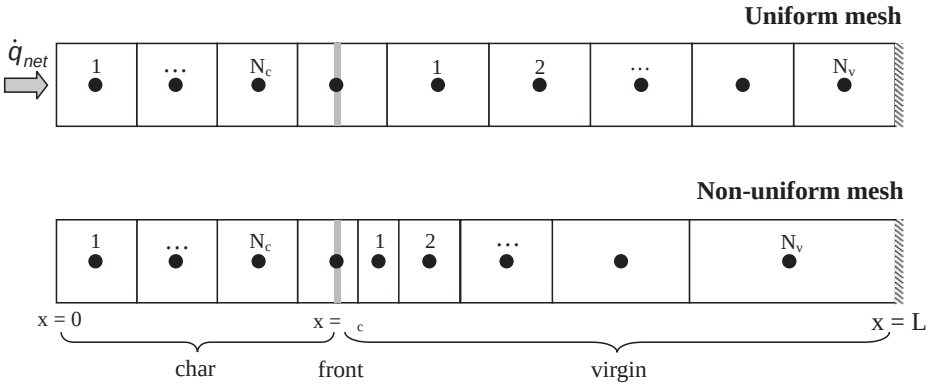

Fig. 1. Example of uniform and nonuniform mesh.

placed on the front [5]. An example of the subsequent mesh for a uniform and a nonuniform mesh in the virgin layer is given in Fig. 1. The grid in the char layer is always kept uniform because the temperature varies almost linearly in this zone.

As was already done for a whole char layer, the conservation of energy can be applied to a single cell:

$$\frac{\mathrm{d}}{\mathrm{d}t}\int_{\Delta x_i} \rho c T \,\mathrm{d}x + \dot{m}''_{\mathrm{g}} c_{\mathrm{g}}(T_{\mathrm{W}} - T_{\mathrm{E}}) + (\rho c)(w_{\mathrm{W}} T_{\mathrm{W}} - w_{\mathrm{E}} T_{\mathrm{E}}) = \dot{q}''_{\mathrm{E}} - \dot{q}''_{\mathrm{W}}, \tag{7}$$

where T_{W} and T_{E} are the temperatures, and w_{W} and w_{E} the boundary velocities at west and east boundary, respectively. The velocity of the mesh boundaries for a volume i is determined by the front velocity and the location of the mesh boundaries. When stretching is used in the virgin layer, the size of a cell is equal to the length of the previous cell multiplied by a growth factor a. The factor is kept constant during the simulation.

3.2. Time discretization

At the transition from the pure heating to the pyrolysis phase, the model equations are singular because the char zone does not yet exist. The problem of solving this singularity is tackled by taking a first order fully implicit time step, only for the first time step in the pyrolysis phase. For the subsequent time steps, the second order accurate Cranck–Nicolson method is used. To calculate a new time step at $n+1$, Eq. (7) is written out at time level $n+\theta$:

$$\rho c \frac{T^{n+1}\Delta x^{n+1} - T^{n}\Delta x^{n}}{\Delta t} + \rho c (T_{\mathrm{W}}^{n+\theta} w_{\mathrm{W}}^{n+1/2} - T_{\mathrm{E}}^{n+\theta} w_{\mathrm{E}}^{n+1/2})$$
$$+ (\dot{m}_{\mathrm{g}}'')^{n+1/2} c_{\mathrm{g}} (T_{\mathrm{W}}^{n+\theta} - T_{\mathrm{E}}^{n+\theta}) = \lambda \left(\frac{\mathrm{d}T}{\mathrm{d}x}\right)_{\mathrm{W}}^{n+\theta} - \lambda \left(\frac{\mathrm{d}T}{\mathrm{d}x}\right)_{\mathrm{E}}^{n+\theta}. \tag{8}$$

For the first pyrolysis time step, which is fully implicit, θ should be taken unity (backward Euler method), otherwise it is $\frac{1}{2}$ (Cranck–Nicholson).

3.3. Solution of discretized equations

The discretized equations for the char or virgin zone result in a tridiagonal matrix. This matrix is solved with the Thomas algorithm [1]. The global solution is obtained with an iterative method. In successive iterations the velocity of the pyrolysis front is corrected until the heat flux balance for the front is satisfied.

Convergence is determined by all node temperatures. When the difference of the node temperatures in successive iterations becomes smaller than a prescribed percentage of the actual node values, the time step is considered to be converged. Differences should be smaller than 10^{-5} percent. If larger, the time of extinction is predicted wrongly. The peak in the mass flux of pyrolysis gases is still predicted well for a 10^{-2} percent convergence criterion, but the time of extinction is strongly overpredicted due to the accumulation of the error in the released pyrolysis gases during the simulation.

3.4. Number of volumes and size of the time step

The number of volumes in the char and virgin layer and the time step length have been varied to find the optimal combination. When less volumes and larger time steps are used, less calculation time is needed.

For the uniform grid in the virgin layer, a grid converged solution was obtained for only four volumes in the char layer and 64 in the virgin material. During pyrolysis the temperature profile in the char layer is almost linear so few cells are needed. On the other hand, the temperature profile in the shrinking virgin layer is better described by an error function [3], so more cells are required. For the material properties used, the time step should be about 0.1 s.

In the nonuniform grid fewer cells are used in the virgin layer. The temperature is varying a lot near the pyrolysis front, thus the volumes should be small in that zone. Further away, the volumes can be larger. Simulations showed that with only 16 cells in the virgin layer a grid converged solution could be obtained. The mesh growth factor was 1.2.

4. Integral model

Instead of solving Eqs. (1) and (3) with a finite volume technique, it is also possible to solve them with a prescribed temperature profile. A linear or quadratic profile for the char layer, and an exponential [6] or quadratic profile [9] for the virgin layer can be used. With the boundary conditions and the conservation equations of energy for the virgin and char zone, the unknown coefficients of the temperature profiles can be derived. The problem can be reduced to a system of three differential equations in three unknowns. In literature, this method is known as the integral model. Details about the integral model can be found in the work of Moghtaderi et al. [9]. The moving grid model will be compared with an integral model where in the char and in the virgin layer a quadratic temperature profile is used. Four cases, with different external heat fluxes, are examined. All cases tend to represent a realistic event, typical for enclosure fires.

Table 1
Material properties [8]

ρ_v (kg/m^3)	ρ_c (kg/m^3)	c_v (J/kg K)	c_c (J/kg K)	λ_v (W/m K)	λ_c (W/m K)	ΔH_{pyr} (J/kg)	T_{pyr} (°C)
650	350	1257	1257	0.1257	0.1257	7.54×10^5	300

The integral model has already been compared with experimental data [9,10]. However, this comparison is hampered by the modelling of the experiment and by the uncertainty of the material properties. Therefore, the difference between the experimental results and the simulation can be due to the approximations made by the integral model or due to the representation of the experiment. When the integral model is compared with the moving grid method, a true mathematical validation is possible because both use the exact same physical model, the same material properties, and the same boundary conditions.

5. Results

In a real fire the incident heat flux can originate from an external heat source, flames at the solid surface, a hot gas layer, etc. In this paper, the simulations are done with a stand-alone model. Therefore, the net incident heat flux has to be supplied as a boundary condition. When the solid model is coupled with a CFD code, this net incident heat flux is computed by the code.

The material parameters that were used in the simulations are given in Table 1. The emissivity of the solid was assumed equal to 1. The thickness of the solid was in all cases 3 cm.

5.1. Sudden increase at start of pyrolysis: Case 1

As soon as in the simulation the pyrolysis starts and combustible volatiles are released (after 12 s in the moving grid model) the external heat flux is raised from 30 to 50 kW/m^2. The constant heat flux of 30 kW/m^2 represents the radiation from remote flames or from test radiation panels. The increase in the incident heat flux represents the ignition of the combustible volatiles in the gas phase. The induction time to obtain an ignitable mixture in the gas phase, is neglected.

Both models give similar results. There are minor differences in the peak of the mass flux of pyrolysis gases (less than 2.5%) and the time at which this peak occurs (about 8%). See Case 1 in Fig. 2.

5.2. Sudden increase at fixed time: Case 2

For enclosed fires, flashover can occur. When a flashover takes place, all the exposed combustible items in the enclosure get involved. This is modelled here as a sudden rise in the external heat flux 60 s after the start of the simulation. In reality, the time of flashover depends on the enclosure conditions. When the external heat flux rises, a char layer has already been formed. Because of the insulating effect of the char layer the peak in the release of pyrolysis gases is now much lower than in Case 1. The integral model shows some peculiar behaviour: immediately after the rise of

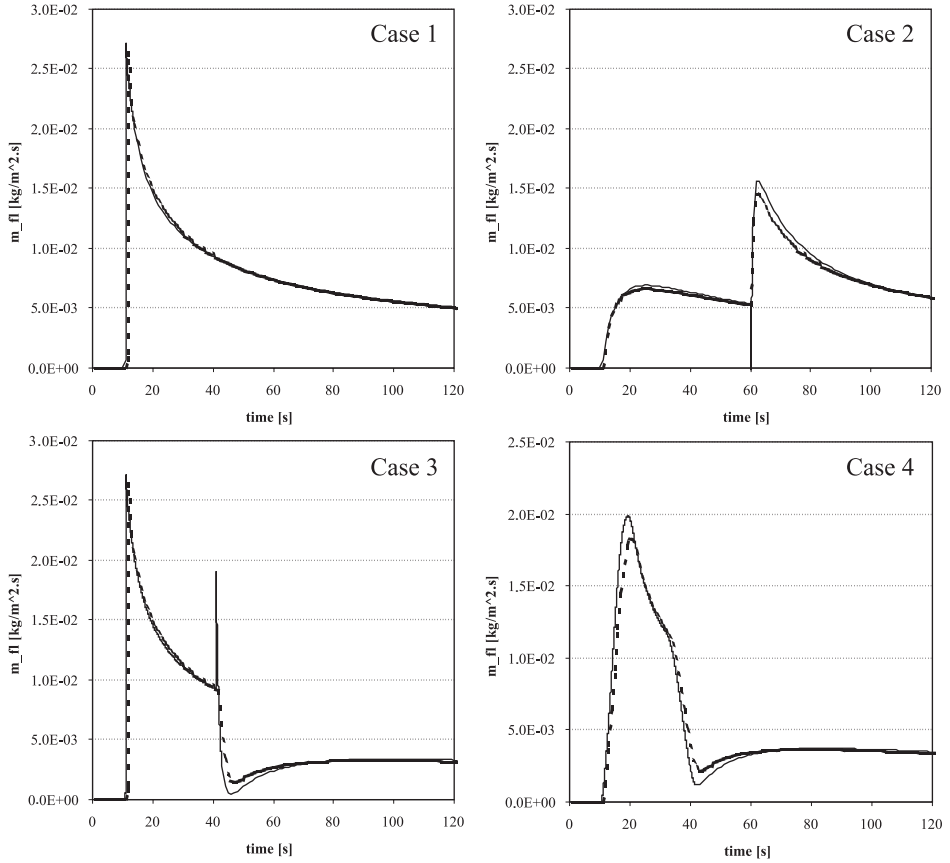

Fig. 2. Mass flux of pyrolysis gases; integral (—) moving grid (- -).

the external heat flux the mass flux of pyrolysis gases drops sharply, see Case 2 in Fig. 2. In some cases even negative mass fluxes were noted. The reason is the unrealistic, direct influence of the net incident heat flux on the whole temperature profile. This sudden decrease in the mass flux of pyrolysis gases is not present in Case 1 as the change in the external heat flux happened just at the start of pyrolysis.

5.3. Sudden increase and fall: Case 3

In this case a sudden rise and fall of the external heat flux is examined. The rise in the external heat flux starts at the beginning of pyrolysis, while the fall occurs at a fixed time. The fall in the external heat flux can represent the extinction of the flames in the gas phase due to e.g. lack of oxygen, or the activation of a sprinkler installation.

Again the integral model gives bad predictions just after the fall of the external heat flux. There is a sudden rise in the mass flux of pyrolysis gases, but less than a second later, the mass flux is normal again, see Case 3 in Fig. 2.

5.4. Smooth increase and fall: Case 4

It is clear that the integral model has problems with sudden changes in the external heat flux. Therefore, in this case, the external heat flux is varied smoothly (sinusoidal for the variation between 30 and 50 kW/m^2).

As can be seen in Case 4 in Fig. 2, when a smooth variation in the external heat flux is applied, the integral model shows good agreement with the moving grid model. The error in the peak of the mass flux of pyrolysis gases is about 8%.

When calculation times are compared, the integral model is in general about 5 times faster than the moving grid model. When a coarse mesh and larger time steps are taken, the calculation time of the moving grid model will of course decrease, but the results will be less accurate.

5.5. Deficiencies of the integral model

The integral model performs very well when the boundary conditions are constant or changing slowly. Sudden changes in the net incident heat flux though, are felt immediately and unrealistically high through the entire solid.

As the temperature is prescribed (e.g. quadratic), the integral model can only be valid for those types of heating that will result in that prescribed temperature profile. In flame spread simulations the incident heat flux can suddenly rise due to for example ignition of the pyrolysis gases in the gas phase, but it can also suddenly fall due to for example lack of oxygen in the gas phase. This kind of heating can result in temperature profiles that are different from the assumed quadratic ones and cannot be described by the integral model.

As the moving grid model permits grid refinement it will converge to the correct solution of the model equations. The integral model on the other side has not the capability to refine and consequently will always give an approximate solution of these model equations.

A last advantage of the moving grid model is the possibility to expand the method to two or three dimensions. In the integral model only one dimensional heat transfer is allowed and thus a more dimensional pyrolysis problem can only be solved as a series of independent one dimensional problems.

6. Conclusion

A moving grid technique has been developed for the solution of the one dimensional pyrolysis of charring solids. Of the two grids examined, the nonuniform is preferred above the uniform. About 4 times fewer cells are needed for the nonuniform grid which results in calculation times that are about 3 times shorter. The growth factor in the nonuniform grid can be taken very large. Values up to 1.2 are still acceptable. In the char layer few cells are required because of the almost linear temperature profile.

Integral models are not always capable of giving correct or realistic results. Sudden changes in the boundary conditions can give temporarily unrealistic results, though the integral model recovers quickly. When large time steps are taken, these effects can be camouflaged.

Errors in the mass flux of pyrolysis gases are largest for sudden changes in the external heat flux and at peak values of the mass flux. For smooth variations of the external heat flux, the maximum peak errors are about 8 percent.

References

[1] D.A. Anderson, J.C. Tannchill, R.H. Pletchen, Computational Fluid Mechanics and Heat Transfer, Hemisphere, Washington, DC, 1984, p. 599.
[2] F.S. Blomshield, J.R. Osborn, Effect of variable solid phase thermal properties on propellant combustion, Acta Astronautica 12 (12) (1985) 1017–1025.
[3] H.S. Carslaw, J.C. Jaeger, Conduction of Heat in Solids, Oxford University, London, 1959, p. 510.
[4] N.S. Cohen, D.A. Flanigan, Mechanisms and models of solid-propellant burn rate temperature sensitivitiy—a review, AIAA J. 23 (10) (1985) 1538–1547.
[5] D.R. Croft, D.G. Lilley, Heat Transfer Calculations Using Finite Difference Equations, Applied Science, Barking, 1977, p. 283.
[6] M.M. Delichatsios, M.K. Mathews, M.A. Delichatsios, An upward fire spread and growth simulation, Fire Safety Science—Proceedings of the Third International Symposium, Edinburgh, 1991, Interscience Communications, London, pp. 207–216.
[7] C. Di Blasi, Processes of flames spreading over the surface of charring solid fuels: effects of fuel thickness, Combust. Flame 97 (1994) 225–239.
[8] A.I. Karpov, V.K. Bulgakov, Prediction of the steady rate of flame spread over combustible materials, Fire Safety Science—Proceedings of the Fourth International Symposium, Ottawa, 1994, Interscience Communications, London, pp. 373–384.
[9] B. Moghtaderi, V. Novozhilov, D. Fletcher, J.H. Kent, An integral model for the transient pyrolysis of solid materials, Fire Mater. 21 (1997) 7–16.
[10] M.J. Spearpoint, J.G. Quintiere, Predicting the burning of wood using an integral model, Combust. Flame 123 (2000) 308–324.
[11] J.E.J. Staggs, A simple model of polymer pyrolysis including transport of volatiles, Fire Safety J. 34 (2000) 69–80.
[12] A. Tewarson, in: SFPE Handbook of Fire Engineering, 2nd Ed., Society of Fire Protection Engineers, Boston, MA, 1995, pp. 3.124–3.53.
[13] Z. Yan, G. Holmstedt, CFD simulation of upward flame spread over fuel surface, Fire Safety Science—Proceedings of the Fifth International Symposium, Melbourne, 1997, Interscience Communications, London, pp. 345–356.